ACCOUNTS
of chemical research

Exploiting Core–Shell Synergy for Nanosynthesis and Mechanistic Investigation

HONG WANG, LIYONG CHEN, YUHUA FENG, AND HONGYU CHEN*

Division of Chemistry and Biological Chemistry, Nanyang Technological University, Singapore 637371

RECEIVED ON JANUARY 27, 2013

CONSPECTUS

The core–shell nanoparticle structure, which consists of an inner layer "guest" nanoparticle encapsulated inside another of a different material, is the simplest motif in two-component systems. In comparison to the conventional single-component systems, complex systems pose both challenges and opportunities. In this Account, we describe our recent progresses in using core–shell motif for exploring new and sophisticated nanostructures. Our discussion is focused on the mechanistic details, in order to facilitate rational design in future studies. We believe that systematic development of synthetic capability, particularly in complex and multifunctional systems, is of great importance for future applications.

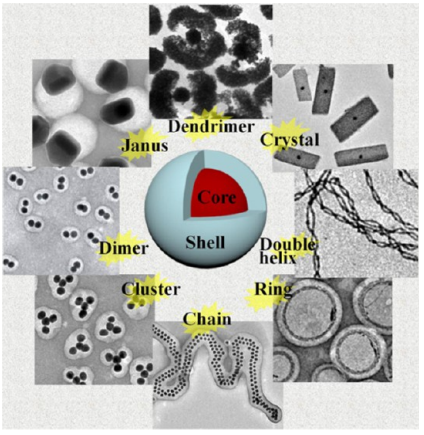

A key issue in obtaining core–shell nanostructures is minimizing the core-shell interfacial tension. Typically, one can coat the core with a ligand for better interaction with the shell. By selecting suitable ligands, we have developed general encapsulation methods in three systems. A variety of nanoparticles and nanowires were encapsulated using either amphiphilic block copolymer (polystyrene-*block*-poly(acrylic acid)), conductive polymer (polyaniline, polypyrrole, or polythiophene), or silica as the shell material.

Obvious uses of shells are to stabilize colloidal objects, retain their surface ligands, prevent particle aggregation, or preserve the assembled superstructures. These simple capabilities are essential in our synthesis of surface-enhanced Raman scattering nanoprobes, in assigning the solution state of nanostructures before drying, and in developing purification methods for nano-objects. When it is applied in situ during nanocrystal growth or nanoparticle assembly, the intermediates trapped by shell encapsulation can offer great insights into the mechanistic details.

On the other hand, having a shell as a second component provides a window for exploring the core–shell synergistic effects. Hybrid core–shell nanocrystals have interesting effects, for example, in causing the untwisting of nanowires to give double helices. In addition, partial polymer shells can bias nanocrystal growth towards one direction or promote the random growth of Au dendritic structures; contracting polymer shells can compress the embedded nanofilaments (Au nanowires or carbon nanotubes), forcing them to coil into rings. Also, by exploiting the sphere-to-cylinder conversion of block copolymer micelles, the Au nanoparticles pre-embedded in the polymer micelles can be assembled into long chains.

Lastly, shells are also very useful for mechanistic studies. We have demonstrated such applications in studying the controlled aggregation of nanoparticles, in probing the diffusion kinetics of model drug molecules from nanocarriers to nanoacceptors, and in measuring the ionic diffusion through polyaniline shells.

1. Introduction

In comparison to the modern chemistry and chemical industry, the field of nanoscience and nanotechnology is still at its infancy. A major bottleneck is the maturity in the synthesis of nano-objects. The field demands synthetic methods that are more reproducible, scalable, versatile, rational, and yield more complex structures with a broader scope.

In the past few decades, geometries such as sphere, cube, wire, and plate have been extensively studied. Notwithstanding these successes, the morphological variety of nanomaterials is still very limited. Without synthetic dexterity of building blocks, it would be nearly impossible to design sophisticated superstructures. In biology, the complex interactions and mechanisms are supported by the rich

Published on the Web 04/24/2013 www.pubs.acs.org/accounts
10.1021/ar400020j © 2013 American Chemical Society

structural variety of biomolecules. In macroscopic world, hardly any machine or device is made of components with basic shapes. Even simple nuts and bolts are too complex from the point of view of nanostructure synthesis.

In terms of designing geometries beyond simple spheres, there are to date only two main origins: crystals and polymers. The shapes of nanocrystals are mostly controlled by their facets. By favoring specific facets, one can obtain a variety of simple geometries such as cube, rod, and octahedron.[1,2] On the other hand, polymer micelles are known to display many morphologies such as sphere, cylinder, toroid, vesicle, and compound structures.[3,4] Both fields have been extensively studied. Exploring their intersection is an effective strategy for exploring new structures and synthetic pathways.

There are only a few ways to combine nanocrystals and polymers. One can encapsulate one component in another, or place two components side by side. The former can be classified as a core–shell structure whereas the latter as a Janus (two-faced) structure. With precise structural control, combining different materials is an effective way to explore their synergistic effects. In our laboratory, we study the formation of core–shell and Janus structures, so that we can design sophisticated nanostructures on the basis of the mechanistic understandings.

In general, the potential energy landscape of multicomponent systems is much more complex than that of single-component ones. While this richer landscape poses great synthetic challenges, it can offer opportunities to achieve structures that are beyond the conventional systems. Given the complex nature of such systems, understanding the underlying mechanisms becomes essential for rational design and synthesis. This Account aims to summarize the key mechanisms related to core–shell nanostructures and their synthetic applications (Figure 1).

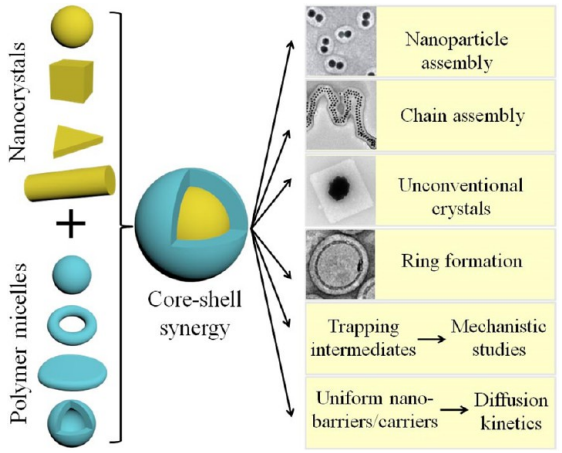

FIGURE 1. Schematics highlighting the strategy for synthetic development and mechanistic studies as discussed in this Account.

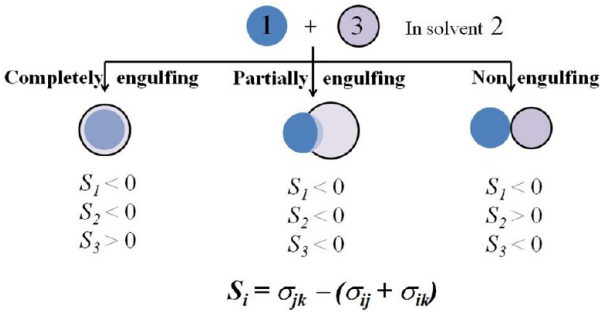

FIGURE 2. Equilibrium configurations for two immiscible liquid droplets 1 and 3 in solvent 2. Reproduced with permission from ref 5.

2. Analysis of Two-Component Nanostructures

In 1970, Mason and Torza used an optical microscope to study the possible conformations of two immiscible droplets in a third immiscible liquid.[5] In general, when combining two phases (1 and 3) in a medium 2, three interfaces are formed (Figure 2); their interfacial energies can be expressed as σ_{12}, σ_{23}, and σ_{13} (all are positive; phase 1 is selected such that $\sigma_{12} > \sigma_{23}$). Depending on their relative strength, droplet 3 can completely, partially, or not engulf droplet 1. The conditions for these scenarios are listed in Figure 2, where $S_i = \sigma_{jk} - (\sigma_{ij} + \sigma_{ik})$ are the spreading coefficients. Simply put, if droplet 1 "hates" solvent 2 ($\sigma_{12} > \sigma_{23} + \sigma_{13}$), it would be more favorable for droplet 3 to completely engulf droplet 1. If droplet 1 "hates" droplet 3 ($\sigma_{13} > \sigma_{12} + \sigma_{23}$), engulfing cannot occur. In between these two extremes, droplet 3 partially engulfs droplet 1 to minimize the overall interfacial energies.

Because the above analysis is based on geometric considerations[5] and the interfacial energies are always proportional to the interfacial area, the analysis is independent of the size of the phases. Thus, the formation of core–shell and Janus nanostructures can be similarly analyzed and even rationally controlled.[6] Though it is often difficult to measure the interfacial energies at nanoscale, they can be qualitatively tuned by adjusting the lattice match/mismatch of the two materials, the hydrophilicity/hydrophobicity of the surface ligands (or of the interfacial surfactants), and the ligand density.

In this analysis, at least one of the phases should flow freely, so that the final configuration can settle in a thermodynamically stable state as dictated by the conditions set in Figure 2. When both phases are solid, the obtained

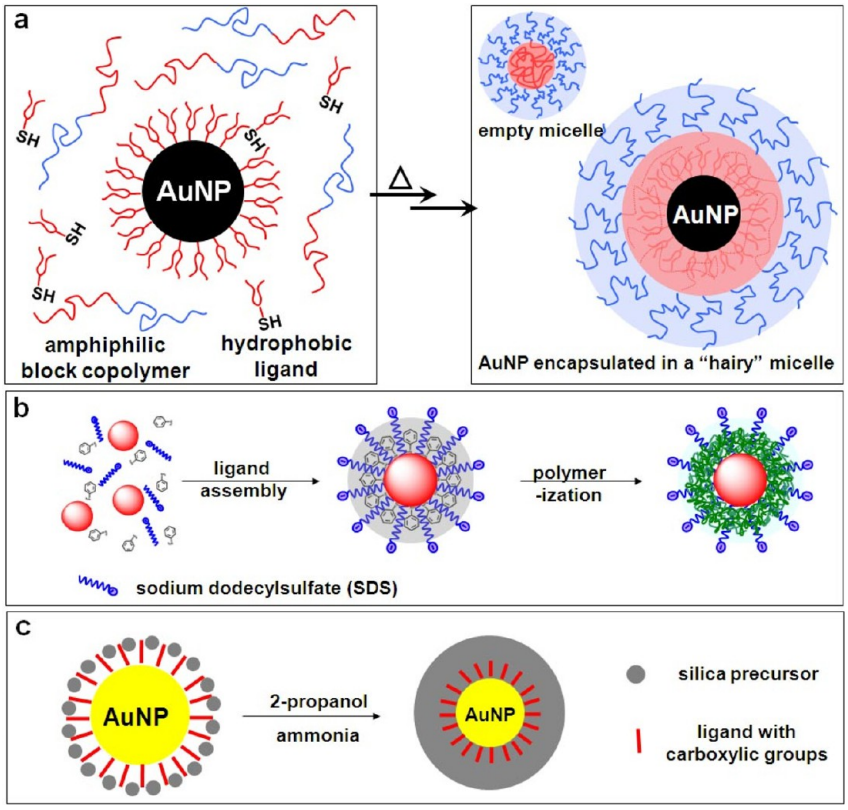

FIGURE 3. Schematics showing the three core–shell systems used in our studies, involving shells of (a) amphiphilic block copolymers; (b) conductive polymers; and (c) silica. Panels (a) and (b) reprinted with permission from refs 8 and 11, respectively. Copyright 2008 Wiley-VCH Verlag GmbH & Co and 2009 the Royal Society of Chemistry.

configuration is not necessarily at the minimal-energy state. The kinetic pathways leading to the nanostructures can also play an important role. The most stable conformations may arise either because the structure eventually reaches equilibrium, or because its formation always follows a minimal-energy pathway.

3. Basic Core–Shell Systems

Core–shell structure has been extensively studied and summarized in several recent reviews.[7] From the point of view of interfacial energies, the key issue is to exchange the surface ligands on the core nanoparticles (NPs), so that the subsequently formed shell can form a wetting layer around the core.

3.1. Shells of Amphiphilic Block Copolymers. The self-assembly of amphiphilic block copolymers has been extensively studied, particularly for polystyrene-*block*-poly(acrylic acid) (PSPAA).[4] In a polar solvent, the polystyrene (PS) blocks tend to aggregate to minimize their contact with solvent. But the resulting micelle cannot grow indefinitely because the tethered poly(acrylic acid) (PAA) blocks strongly repel one another. The micelle formation is similar to that of small surfactant molecules. If any NP can be functionalized with a suitable hydrophobic ligand, it would be possible to self-assemble the polymer around it forming core–shell structures (Figures 3a, 4a–d).[8]

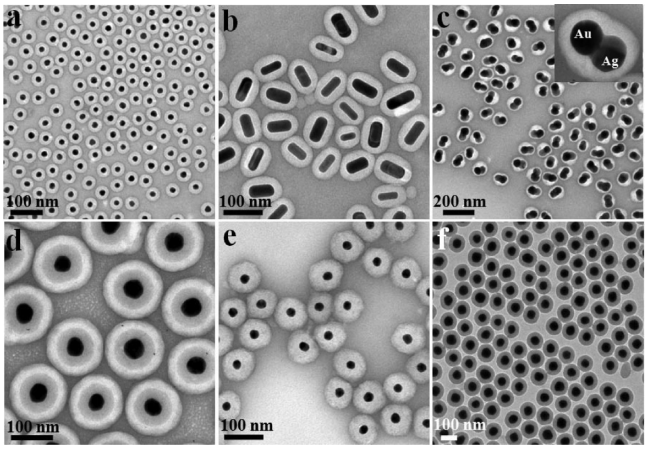

FIGURE 4. TEM images of typical core–shell nanostructures: (a) AuNP@PSPAA; (b) (Au nanorod)@PSPAA; (c) (Au–Ag dimer)@PSPAA; (d) multilayer (Au@SiO_2)@PSPAA; (e) AuNP@PANI; (f) AuNP@SiO_2. Panels (d) and (e) reprinted with permission from refs 15 and 11, respectively. Copyright 2012 Wiley-VCH Verlag GmbH & Co and 2009 the Royal Society of Chemistry.

In the conventional approach, the self-assembly of amphiphilic block copolymer is induced by the slow addition of a nonsolvent (e.g., water) to a polymer solution in a good solvent (e.g., DMF).[4] The gradual decrease in solubility causes the polymer to be excluded from the solution, forming micelles. Using this approach, Taton and co-workers pioneered the encapsulation of several types of NPs in cross-linked PSPAA shells.[9] In our works, NPs are directly mixed with PSPAA in a precise solvent mixture (e.g., DMF/water = 4:1), so that the polymer can assemble under optimized conditions for sufficient time.[3,8] Thus, the method is facile, scalable, and reproducible. After the assembly, quick addition of water can remove DMF from the polymer domain, deswelling it and locking the resulting nanostructure.

In general, the use of hydrophobic ligands is critical for tuning the NP–PS interfacial energy for giving core–shell structure. During PSPAA self-assembly, the PS blocks are adsorbed on the ligand-coated NP surface, driven by van der Waals and hydrophobic interactions. The PS domain is highly swollen by DMF, and thus, it is sufficiently mobile to adopt a minimal-energy conformation with respect to the NP.

Like in empty micelles, the size of the polymer shells is limited by the repulsion among the PAA blocks. Moreover, the PS domain is limited in thickness by the physical length of the PS blocks, which are entropically unfavorable when stretched. Thus, the shell thickness is thermodynamically controlled; that is, shells too thick or too thin are unstable.

3.2. Shells of Conductive Polymers. Typical conductive polymers include polyaniline (PANI),[11] polypyrrole (PPy),[10,11] and polythiophene (PTh).[12] They can be easily synthesized by the direct polymerization of the respective monomers, but the resulting polymer chains do not repel one another. Thus, directly encapsulating NPs by in situ polymerization often leads to aggregation.

Our group developed a simple approach by introducing a surfactant, sodium dodecylsulfate (SDS). The monomers were polymerized in situ in the presence of NPs and SDS. The following is a typical example: When aniline adsorbs on the surface of AuNPs, the AuNPs become hydrophobic and tend to aggregate. In the presence of SDS, it self-assembles on the aniline-coated AuNPs, endowing them with negative charges and preventing aggregation. When the oxidant $(NH_4)_2S_2O_8$ is added, aniline is continually oxidized to PANI. Because of the cross-linking of PANI, the polymer domain cannot flow and it grows with the layer-by-layer deposition of PANI, forming core–shell nanostructures (Figures 3b and 4e). Thus, the shell thickness is kinetically controlled, unlike the above PSPAA system.

With modifications, this method can be used to encapsulate a variety of metal NPs in shells of PANI, PPy, or PTh, forming core–shell structures. The oxidant plays an important role because the extent of cross-linking and the hydrophilicity of the polymer depend on the nature of the oxidation reaction.[13]

3.3. Shells of Silica. In addition to polymer, silica has been frequently used for building core–shell nanostructures. It is essentially a highly cross-linked inorganic polymer, but chemically more robust than organic ones. In addition, it is porous and optically transparent.

There are two main methods for depositing silica on the surface of NPs: In the Stöber method, NH_3 catalyzes the hydrolysis of tetraethoxylsilane (TEOS) in a water/alcohol mixture.[14,15] Alternatively, with the help of surfactants, TEOS hydrolysis can occur in the aqueous microdroplets of water-in-oil emulsion.[16] Because the silica domain is highly cross-linked, it cannot flow once it is formed. Thus, silica shell can be continually grown by the layer-by-layer deposition (Figures 3c and 4f); the shell thickness can be easily tuned by modulating the extent of silica formation.

The main issue is to modify the NP surface with a suitable ligand, so that silica can form a wetting layer on the NP surface (i.e., minimizing the NP-silica interfacial energy). In general, ligands should have –Si–OH or –COOH terminal groups to render the NP amenable for silica adsorption (e.g., 3-amino-propyltriethoxysilane or 4-mercaptobenzoic acid). These methods have been well established giving many core–shell NPs.

3.4. Other Core–Shell Nanoparticles. In the metal–metal and semiconductor-semiconductor core–shell NPs, the interfacial energy between the two materials is mainly determined by the extent of their lattice mismatch.[7,17,18] On the other hand, a metal shell can be coated on the surface of oxide or polymer.[19,20] Core–shell systems such as those have a great potential for designing complex structures. For example, coating Pd on a special type of Au–Ag alloy nanowires (NWs) can give double helices.[21]

4. Shells as a Means of Preservation

Colloidal nanostructures can be highly dynamic: ligands are constantly binding and dissociating; crystals are growing and dissolving; NPs are aggregating and separating. Hence, shells can play an important role in preserving the overall structure, which is critical for both characterization and application.

4.1. Preservation of Surface Ligands. In certain applications, for example, surface-enhanced Raman scattering

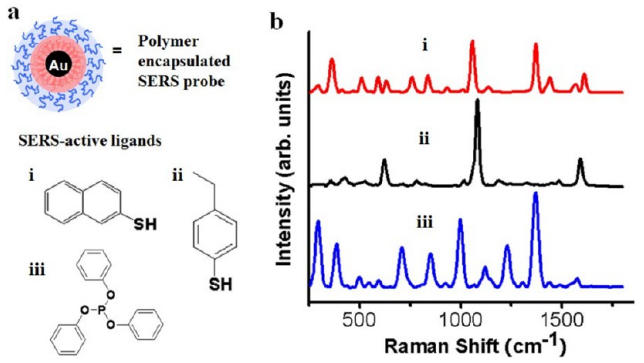

FIGURE 5. (a) Schematics showing the use of different SERS active-ligands for making AuNP@PSPAA SERS nanoprobes; (b) SERS spectra of the respective nanoprobes. Reprinted with permission from ref 23. Copyright 2009 Wiley-VCH Verlag GmbH & Co.

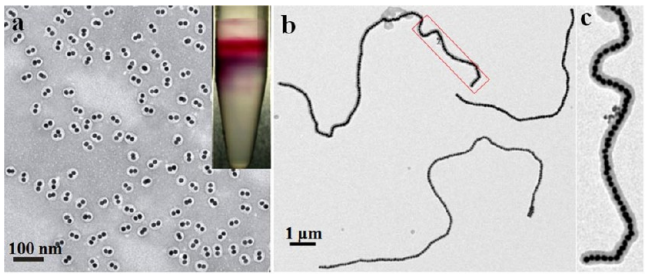

FIGURE 6. (a) TEM image of dimers of AuNPs; inset: photograph showing the separation of dimers from monomers using differential centrifugation. Adapted with permission from ref 28. Copyright 2009 American Chemical Society. (b, c) TEM images of PANI -coated single-line chains of AuNPs after purification. Reprinted with permission from ref 29. Copyright 2011 American Chemical Society.

(SERS), preventing ligand dissociation and exchange is of great importance. The number of ligands on the NPs is a critical factor for their SERS intensity. But over long periods of time, these ligands can dissociate. Even a strong thiol ligand could dissociate from Au surface, not to mention ligands bound by weak interactions. By using a polymer or silica shell,[22,23] the ligands are locked inside the shells and isolated from the environment. We have demonstrated that SERS-active ligands can be used to modify Au/Ag NPs, rendering them amenable for PSPAA encapsulation (Figure 5).[23] Thus, the resulting core–shell NPs can be used as SERS probes. Because the shells ensure the colloidal stability of the NPs, a wider variety of ligands can be used, including weak and insoluble ligands. Moreover, the identical outer surface of these core–shell NPs is amenable for general applications. When using multiple types of SERS NPs, completely preventing ligand exchange among them is a necessity for multiplexed sensing and detection.

4.2. Preservation of Nanoparticles and Their Assemblies. A general problem in characterizing colloidal nanostructures is that the samples have to be dried before being studied by electron microscopy (TEM/SEM). However, the act of drying concentrates NPs as well as salts, often leading to serious aggregation. It is not always clear whether the observed structure is formed in the solution.

With the protection of the shells, the solution form of the NPs can be better preserved. In several cases, we have shown that the act of polymer encapsulation did not cause a significant change in the plasmon absorption spectra of the samples.[11,24] Thus, the solution species can be clearly identified, and the response in SERS or UV–vis signals can be better interpreted. Particularly for SERS studies,[23] knowing the population of the aggregated NPs is essential because the SERS hotspots thereof can have much stronger SERS intensity than the individual NPs. In our group, we demonstrated the purity of nonaggregated NPs[23,25] and of Au–Ag dimers using this shell encapsulation method.[6]

Random aggregation of NPs in a colloidal solution is to a certain degree similar to the polymerization of organic monomers, because the NPs have to find each other via diffusion and random collision, which involves similar principles. We used PSPAA encapsulation to preserve the AuNP assemblies and attempted to fit their "polymerization" kinetics.[26] With the polymer shells preventing aggregation and dissociation, the assemblies can be readily characterized, purified and used for SERS studies.[26–28]

Similarly, shell encapsulation can be applied to larger assembled structures. We developed a new method to assemble NP chains: When freezing an aqueous solution of AuNPs, the NPs were trapped in the ice veins, forming long and nonbranched chains.[29] However, these chains were fragile and easily broken. After in situ polymerization to form PANI coating on the chains, the mechanical strength of the chains was improved, and thus, we were able to isolate and purify the single-line chains (Figure 6b, c).

4.3. Allowing Purification of Nanoparticles. Purification of NPs and their assembly in nanoscience is as important as purification of chemicals in organic chemistry. We discovered that differential centrifugation using high-density CsCl solutions is an effective method for separating NP clusters.[28] However, colloidal NPs are generally not stable in salt solutions. Typical NPs would easily aggregate under physiological salt concentrations (~0.45 mM), not to mention near-saturated CsCl solutions (11 M). After PSPAA encapsulation, the colloidal stability of the resulting core–shell NPs was greatly improved. At pH > 10, their surface is covered with

long ionic PAA chains in an extended conformation, introducing charge and steric repulsion against aggregation. Thus, using PSPAA shells as a means of protection, we were able to purify dimers of AuNPs to about 95% purity (Figure 6a).

This method was further used to prepare dimers and trimers of AgNPs with 85% and 70% purity, respectively. The structural uniformity of the hotspots in these clusters allowed direct SERS measurements of colloidal samples (as opposed to dried samples).[27] This led to improved calculation and interpretation of the respective SERS enhancement factors.

At high temperature, the polymer shells on the purified dimers can be burned away, and the AuNPs can act as catalysts for growing ZnO NWs.[26] This was a proof-of-concept demonstration that the information from colloidal assembly can be retained for vapor–liquid–solid growth of oxide superstructures.

5. Use of Core–Shell Motif for Advanced Nanostructures

With controlled synthesis of core–shell nanostructures, we can build from them more complex structural features. Core–shell NPs possess two components with distinctive properties, both of which can be exploited for unique growth or assembly modes.

5.1. Unconventional Crystal Growth. In comparison to the synthesis of single-component nanocrystals, nucleation and growth of nanocrystals in mutlicomponent systems has been much less studied. The complex interactions among the components are a great challenge in terms of synthetic design. From this perspective, well-controlled core–shell nanostructures are an important step toward complex nanocrystals.

Au–Perylene Hybrid Nanocrystals. We found that a single-crystalline perylene domain can grow around polycrystalline Au seeds, forming hybrid nanocrystals (Figure 7a).[30] This core–shell system was highly unconventional considering the mismatch between perylene lattice and the polycrystalline Au core. PANI encapsulation was used to trap the growth intermediates. It was observed that the perylene crystal initiated from 1–2 locations on the Au seed, and then grew larger, eventually engulfing the entire seed (Figure 7b–e). Thus, it appeared that the perylene crystal can accommodate AuNP and small misoriented perylene domains as defects. We postulated that it was because of the weak and nondirectional van der Waals interactions among perylene molecules, which can tolerate slight distortion or reorientation of a few misaligned molecules during crystal formation.

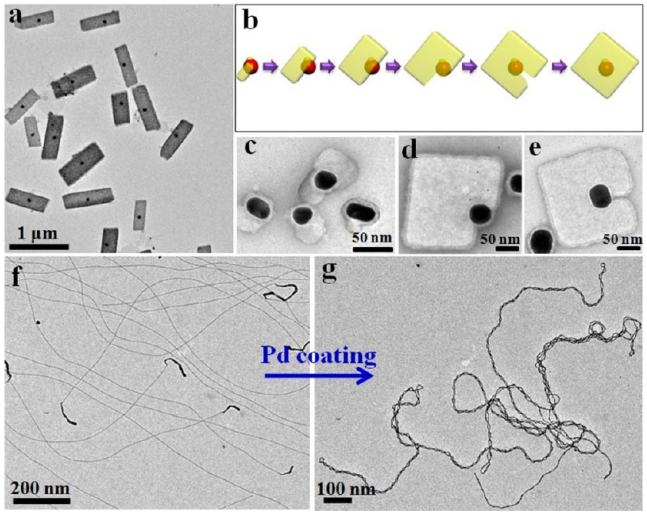

FIGURE 7. (a) TEM image of AuNP@perylene hybrid nanocrystals; (b) schematics of the proposed growth intermediates; (c–e) examples of the PANI-trapped intermediates. Panels (a)–(e) reprinted with permission from ref 30. Copyright 2011 Wiley-VCH Verlag GmbH & Co. TEM images of (f) Au–Ag alloy NWs; and (g) a double helix resulted after coating these NWs with Pd. Adapted with permission from ref 21. Copyright 2011 American Chemical Society.

Nanowire Double Helices. When metal NWs are used as seeds, coaxial core–shell NWs can be obtained. We reported an interesting case where the cores were a special type of Au–Ag alloy NWs (Figure 7f) with a unique twisted structure, namely, Boerdijk–Coxeter–Bernal (BCB) helix.[21] Upon the growth of an additional metal layer (Pd, Au, or Pt), each NW wound around itself to form a double helix (Figure 7g). The product was a mixture of left- and right-handed helices, but within an individual helix the chirality was highly consistent. We proposed that this consistency originated from the highly ordered chiral lattice of the initial Au–Ag alloy NWs. Upon metal deposition, the lattice strain in the NWs increased to a critical level, so that they "want" to convert back from the BCB helix to the conventional fcc structure. This forced the entire wire to untwist, giving a double helix.

Au/Ag Growth in PANI. In the above two cases, the unusual nanocrystals arise from the core–shell structure and the unique combination of materials. In addition, we showed that the presence of PANI shells can greatly influence the deposition of Au/Ag on Au seeds, giving rise to several types of unique crystal growth modes.

When $AgNO_3$ was used to oxidize aniline in the presence of Au seeds, the partially oxidized PANI domains acted like a liquid. They were able to move to one side of the Au seeds,

forming Janus NPs (Figure 8a).[13] While Ag can diffuse through the PANI domains and grow epitaxially on the Au seeds, the growth was highly anisotropic because of the eccentricity of the PANI domains (Figure 8b). Thus, the partial shells provided a means to break the symmetry in the growth of nanocrystals.

In contrast, when $HAuCl_4$ was used as an oxidant, the resulting PANI was highly cross-linked. Once a PANI domain was formed, it cannot move on the Au seed. However, the subsequent Au deposition was dependent on the size and shape of the PANI domain.[31] As a result, the Au growth was branching and chaotic. Controlled by the diffusion of $AuCl_4^-$ and aniline, the extending branches on the Au seeds eventually gave fractal nanostructures. Using this methodology, 3D dendritic nanostructures (Figure 8c) were synthesized in colloidal solutions[31] and 2D (Figure 8d) ones were synthesized on a substrate surface.[32]

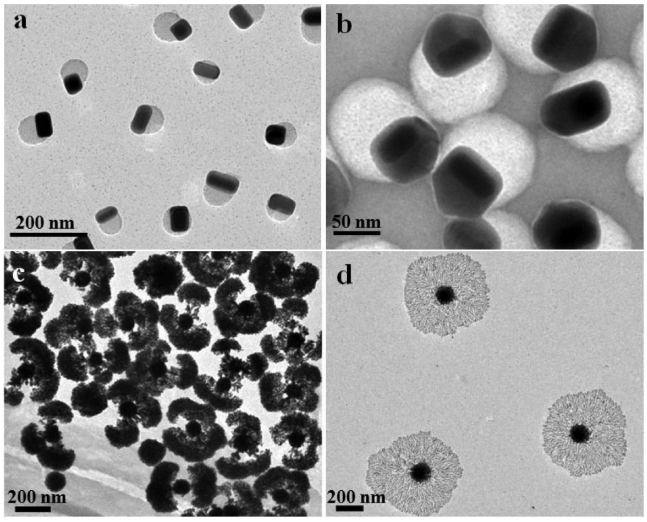

FIGURE 8. TEM images of (a) eccentric (Au@Ag)@PANI NPs synthesized from Au nanrods; (b) the same NPs after extensive Ag growth. Panels (a) and (b) reprinted with permission from ref 13. Copyright 2010 American Chemical Society. (c) 3D and (d) 2D dendritic nanostructures obtained by PANI-induced Au growth. Panel (d) reprinted with permission from ref 32. Copyright 2012 the Royal Society of Chemistry.

5.2. Unconventional Chain Assembly of Nanoparticles. A more interesting application of core–shell motif is to exploit their synergistic effects for nanoparticle assembly. In particular, PSPAA micelles are known to transform from spheres to cylinders upon acid treatment. Using AuNP@PSPAA core–shell NPs as monomers, this transformation induced highly selective linear assembly of the preembedded AuNPs (Figure 9).[33]

Normally, the "polymerization" of colloidal NPs follows the step-growth mode. A general characteristic is that the monomers are quickly consumed and the latter stage was dominated by the aggregation of large clusters. Even when the initial aggregation is highly selective (e.g., linear assembly),[24] the latter stage of aggregating NP chains becomes more difficult and less selective. Thus, it is a great challenge to fabricate long chains (>30 NPs in length) without branching.

To our surprise, the self-assembly of the core–shell AuNP@PSPAA followed an unconventional chain-growth mode. As shown in Figure 9b, after treating AuNP@PSPAA with acid, long chains of AuNPs were obtained. The large amount of residue monomers is a key factor for growing long chains. Obviously, some clusters were able to aggregate many times whereas most of the monomers did not even aggregate once, indicating a unique "polymerization" mode. The long chains can be easily separated from the monomers (Figure 9c).

By controlling the swelling of PS domains (i.e., adjusting the solvent ratio), single-line chains of up to 300 NPs in length were also synthesized. Even prefabricated single-line chains can be converted to double- or triple-line chains, indicating the critical role of PS–solvent interfacial tension in restricting the width of the chains. We deswelled the PS domain by adding water to the solution, thus

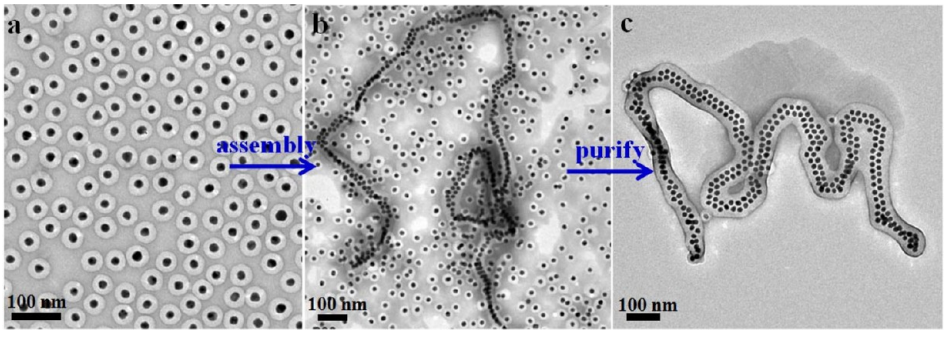

FIGURE 9. TEM images of (a) AuNP@PSPAA monomers; (b) a typical result after assembly; and (c) a purified double-line chain. Reprinted with permission from ref 33. Copyright 2012 Wiley-VCH Verlag GmbH & Co.

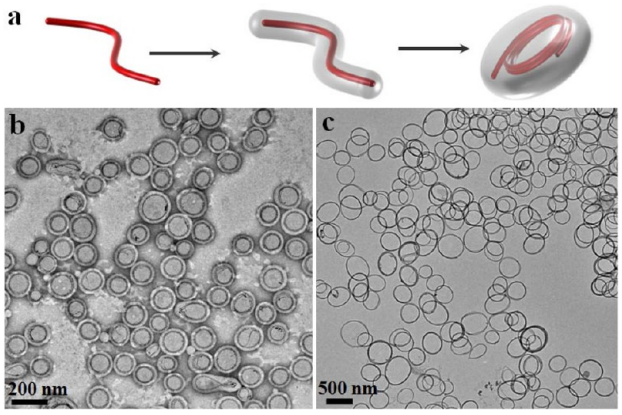

FIGURE 10. (a) Schematics showing the polymer-induced coiling of nanofilament. TEM images of (b) coiled AuNWs embedded in PSPAA shells; and (c) coiled CNT rings after removing PSPAA. Panels (a) and (b) reprinted with permission from ref 34. Copyright 2010 American Chemical Society. Panel (c) reprinted with permission from ref 35. Copyright 2011 American Chemical Society.

trapping aggregation intermediates for detailed mechanistic studies.

5.3. Creating Rings. A further demonstration of core–shell synergy is to exploit the contraction of polymer shells for coiling embedded nanofilaments. Ultrathin AuNWs (d = 1.8 nm) were first encapsulated by PSPAA shells in a DMF/water mixture.[34] After addition of water to cause deswelling, the initially spread-out polymer domains contracted into spheres, forcing the embedded AuNWs to coil into rings (Figure 10a, b). Interestingly, the coiled AuNWs stored mechanical energy in the form of elastic potential energy. Thus, they can spontaneously spring back after the polymer shells were removed.

The same methodology can be used to coil carbon nanotube (CNT) bundles.[35] Owing to the strong stacking among CNTs, the resulting rings did not spring back after removing the polymer shells (Figure 10c). With these robust rings, we demonstrated their reversible compression and expansion. While the elastic energy involved in this process was very small, the underlying principles are similar to the mechanical springs in pens. Following this work, we developed a general methodology of using both oil-in-water and water-in-oil emulsions for coiling several types of nanofilaments.[36]

In any single-component system, it is difficult to create high energy nanostructure because the system energy always decreases. In contrast, two-component core–shell systems offer a rich energy landscape for designing complex structures. While the overall system energy also decreases, the polymer shell can do work to the embedded nanofilamant, forcing the latter to high-energy states.

In a different system, planar spirals were fabricated by coating PTh on AgNWs.[37] The 5-fold twinned AgNWs contained angular misfit defects that occurred on the same face. During the oxidation of thiophene to PTh, the AgNWs were partially etched and the preferred etching of angular misfit defects broke the 5-fold symmetry. As a result, the imbalance of PTh formation at these sites caused the etched AgNWs to consistently bend along a same direction, coiling the Ag@PTh nanocomposites into planar spirals.

6. Use of Core–Shell Motif for Mechanistic Studies

In addition to synthetic development, core–shell motif is also very useful for mechanistic studies. Having two components in a precisely controlled nanostructure can offer many advantages.

6.1. Trapping Intermediates for Mechanistic Study. The simplest use of shells is to trap "reaction" intermediates, that is, if NPs can be preserved in situ during their growth or aggregation. Shell encapsulation is in general much less disruptive than drying as a means of trapping intermediates. With shells, the intermediates can be readily isolated and characterized in nearly the same state as the solution species, permitting mechanistic insights.

An example has been discussed in section 5.1, where PANI encapsulation was used to trap the growth intermediates of perylene nanocrystals.

The ability to trap aggregation intermediates is invaluable for studying the spontaneous linear aggregation of AuNPs.[24] We found that the aggregation was kinetically controlled. Once the AuNPs made contact with each other, their mutual interactions were usually too strong for them to separate. Hence, the critical point in determining the cluster structure occurred at the "transition state", before the NPs met each other, at which point the charge repulsion among the NPs was the dominant factor. For an incoming NP attaching to a dimer/chain, it experiences less charge repulsion via end-on than side-on aggregation, thus favoring the formation of chains (Figure 11a, b).

This methodology can be applied to studying the controlled aggregation of two different types of NPs.[38] A tetrathiol ligand was used to cover AuNPs with thiol groups (type A-NPs); whereas type B-NPs were citrate-stabilized AuNPs since their surface ligands can be easily displaced. Using PSPAA shells to preserve the reaction products, we were able to analyze the reaction outcome, that is, the population of the different-sized clusters. When treating A-NPs

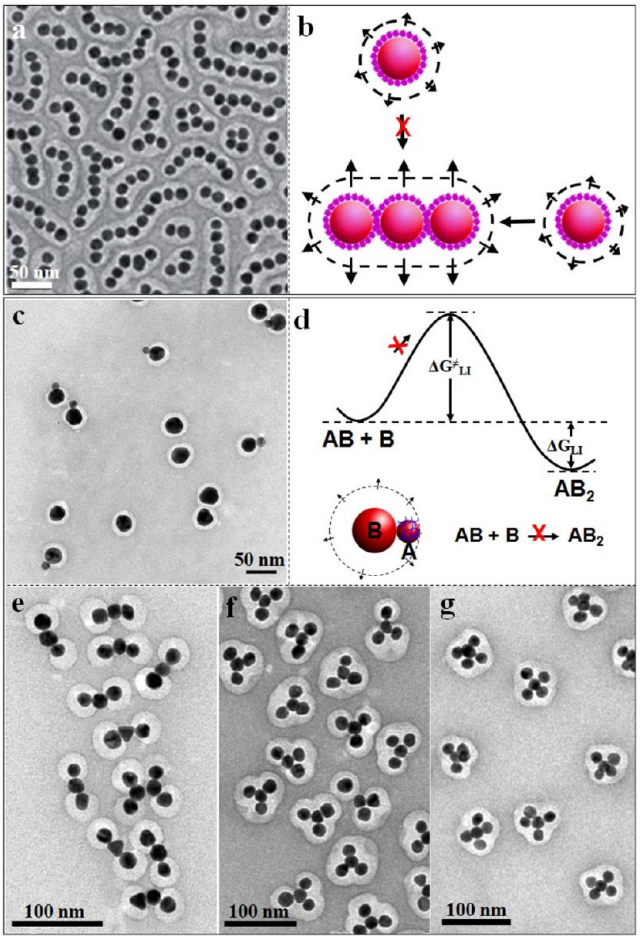

FIGURE 11. (a) TEM image of linear aggregates of AuNPs trapped by PSPAA shells; (b) schematics showing the favored end-on aggregation to a chain. Panels (a) and (b) reprinted with permission from ref 24. Copyright 2010 Wiley-VCH Verlag GmbH & Co. (c) TEM image of AB NPs after PSPAA encapsulation; (d) schematics showing that the charge repulsion (dashed circles with arrows) among B NPs is the main barrier at the transition state; (e–g) TEM images of AB_2, AB_3, and AB_4 nanoclusters. Panels (c)–(g) reprinted with permission from ref 38. Copyright 2010 Nature Publishing Group.

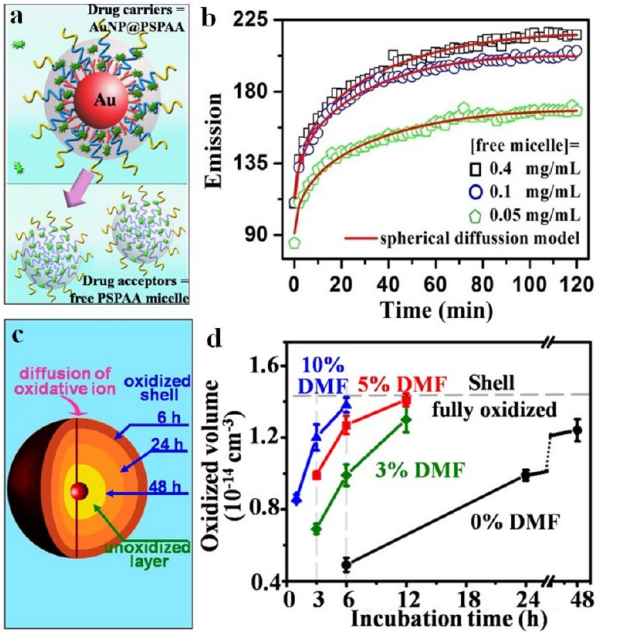

FIGURE 12. (a) Schematics showing the transfer of pyrene (dark-green dots) from the polymer shells of AuNPs to free PSPAA micelles. (b) Fluorescence intensity traces showing the kinetics of pyrene release. Panels (a) and (b) reprinted with permission from ref 39. Copyright 2010 Wiley-VCH Verlag GmbH & Co. (c) Schematics showing the diffusion kinetics of oxidative ions through the OANI shell causing its cross-linking. (d) Effects of swelling on the ionic diffusion, showing a plot of the oxidized PANI volume against the incubation time. Panels (c) and (d) reprinted with permission from ref 40. Copyright 2012 American Chemical Society.

with excess amount of B-NPs, one would expect the A-NPs to be fully surrounded by many B-NPs. Surprisingly, the stoichiometry of the resulting cluster was independent of the A:B ratio. We found that the nanoreaction was kinetically controlled and that the charge repulsion among the B-NPs was a key factor in the "activation barrier" at the "transition state" (Figure 11c, d). Thus, the stoichiometry was highly dependent on the ionic strength of the media. The resulting clusters can be easily purified to give stoichiometry-controlled products (Figure 11e–g).

6.2. Studying the Kinetics of Short-Distance Drug Release. A main difficulty in studying drug release is to distinguish the loaded drug molecules from those released. We developed a model delivery system (Figure 12a),[39] where the pyrene molecules loaded in AuNP@PSPAA were quenched in fluorescence by the Au core. Thus, upon releasing, the fluorescence reemerged and the unloaded molecules can be quantified to study their diffusion kinetics. The core–shell NP was highly uniform in structure, providing both a "cargo bay" and a fluorescence quencher. The NPs can be dispersed in a solution to form an intimate mixture with the nanoacceptors. This creates a reliable model system for studying the short-distance (<1 μm) drug release between two homogeneously suspended entities.

As shown in Figure 12b, the temporal evolution of fluorescence can be nicely fit to the Fickian diffusion model. The presence of nanoacceptors at short-range greatly facilitated the pyrene release from the nanocarriers. This is not surprising considering the macroscopic diffusion distance in the conventional models (e.g., dialysis). The nanoacceptors were varied from simple SDS micelles, to bovine serum albumin, and to mimics of a cell membrane (micelles of phospholipid). The kinetic behavior of pyrene release was very similar in all cases. Moreover, because PSPAA micelles are kinetically frozen in aqueous solution and they do not aggregate even

in concentrated CsCl solution, we were able to determine the exact diffusion pathway of the released pyrene molecules.

6.3. Studying Ionic Diffusion in PANI. We discovered that the oligoaniline (OANI) shells on AuNPs can be partially oxidized by $HAuCl_4$ to PANI. The unreacted section can be selectively dissolved to give yolk-shell nanostructures (Figure 12c).[40] Thus, in this core–shell system, the extent of partial shell oxidation can be quantified to reveal the extent of $AuCl_4^-$ diffusion. The oxidized domains were uniform in thickness, indicating the absence of irregular pores in the original shells. The uniform nanoscale shells provide a better platform than bulk membranes, where a small amount of defects or large pores may contribute dominantly to the diffusion of ionic species.

The rate of $AuCl_4^-$ diffusion in the nanoscale PANI shells was estimated to be about 700 times slower than the typical rates measured from bulk membranes. Thus, in the absence of irregular/large pores, the intrinsic diffusion rates can be more reliably determined. Swelling the polymer shells by organic solvents (e.g., DMF) can be used to modulate the pores in the polymer, thus facilitating ionic diffusion (Figure 12d). Hence, the nanoscale core–shell nanostructures provide a model system for evaluating the effects of pores in ionic diffusion.

7. Summary

In this Account, we summarized the principles of fabricating core–shell nanostructures and demonstrated the exploitation of core–shell synergy for synthetic developments as well as fundamental studies. In comparison to the single-component systems, core–shell systems are more complex. Such a system requires more understanding but it can offer new opportunities. As demonstrated above, we can rationally design novel nanostructures and study new fundamental problems. Systematic development of these capabilities is essential for future application of sophisticated nanostructures. In our future study, we aim to improve our understanding of the current systems and to explore more complex systems for new inspirations.

BIOGRAPHICAL INFORMATION

Hong Wang received her B.Sc. and M.Sc. from Anhui Normal University. She is now a Ph.D. candidate under the supervision of Prof. Chen.

Liyong Chen received his Ph.D. from the University of Science and Technology of China, and then spent 3 years with Prof. Chen as a postdoctoral fellow. In 2012, he joined Dalian University of Technology as an Associate Professor.

Yuhua Feng received his Ph.D. from Nankai University. He is now a postdoctoral fellow with Prof. Chen.

Hongyu Chen received his B.Sc. from the University of Science and Technology of China and then his Ph.D. from Yale University. He joined Nanyang Technological University in 2006, where he is now an Associate Professor. His research focuses on the mechanisms underlying the synthesis, assembly, and manipulation of nanostructures.

FOOTNOTES

*To whom correspondence should be addressed. E-mail: hongyuchen@ntu.edu.sg.
The authors declare no competing financial interest.

REFERENCES

1 Grzelczak, M.; Perez-Juste, J.; Mulvaney, P.; Liz-Marzan, L. M. Shape Control in Gold Nanoparticle Synthesis. *Chem. Soc. Rev.* **2008**, *37*, 1783–1791.
2 Xia, Y. N.; Xiong, Y. J.; Lim, B.; Skrabalak, S. E. Shape-Controlled Synthesis of Metal Nanocrystals: Simple Chemistry Meets Complex Physics? *Angew. Chem., Int. Ed.* **2009**, *48*, 60–103.
3 Liu, C.; Chen, G.; Sun, H.; Xu, J.; Feng, Y.; Zhang, Z.; Wu, T.; Chen, H. Toroidal Micelles of Polystyrene-block-Poly(acrylic acid). *Small* **2011**, *7*, 2721–2726.
4 Mai, Y.; Eisenberg, A. Self-assembly of Block Copolymers. *Chem. Soc. Rev.* **2012**, *41*, 5969–5985.
5 Torza, S.; Mason, S. G. Three-Phase Interactions in Shear and Electrical Fields. *J. Colloid Interface Sci.* **1970**, *33*, 67–83.
6 Feng, Y.; He, J.; Wang, H.; Tay, Y. Y.; Sun, H.; Zhu, L.; Chen, H. An Unconventional Role of Ligand in Continuously Tuning of Metal–Metal Interfacial Strain. *J. Am. Chem. Soc.* **2012**, *134*, 2004–2007.
7 Ghosh Chaudhuri, R.; Paria, S. Core/Shell Nanoparticles: Classes, Properties, Synthesis Mechanisms, Characterization, and Applications. *Chem. Rev.* **2012**, *112*, 2373–2433.
8 Chen, H.; Abraham, S.; Mendenhall, J.; Delamarre, S. C.; Smith, K.; Kim, I.; Batt, C. A. Encapsulation of Single Small Gold Nanoparticles by Diblock Copolymers. *ChemPhysChem* **2008**, *9*, 388–392.
9 Kang, Y.; Taton, T. A. Core/Shell Gold Nanoparticles by Self-Assembly and Crosslinking of Micellar, Block-Copolymer Shells. *Angew. Chem., Int. Ed.* **2005**, *44*, 409–412.
10 Xing, S.; Tan, L. H.; Chen, T.; Yang, Y.; Chen, H. Facile Fabrication of Triple-Layer (Au@Ag)@Polypyrrole Core-Shell and (Au@H_2O)@Polypyrrole Yolk-Shell Nanostructures. *Chem. Commun.* **2009**, 1653–1654.
11 Xing, S.; Tan, L. H.; Yang, M.; Pan, M.; Lv, Y.; Tang, Q.; Yang, Y.; Chen, H. Highly Controlled Core/Shell Structures: Tunable Conductive Polymer Shells on Gold Nanoparticles and Nanochains. *J. Mater. Chem.* **2009**, *19*, 3286–3291.
12 Sun, H.; He, J.; Xing, S.; Zhu, L.; Wong, Y. J.; Wang, Y.; Zhai, H.; Chen, H. One-step Synthesis of Composite Vesicles: Direct Polymerization and in situ Over-Oxidation of Thiophene. *Chem. Sci.* **2011**, *2*, 2109–2114.
13 Xing, S.; Feng, Y.; Tay, Y. Y.; Chen, T.; Xu, J.; Pan, M.; He, J.; Hng, H. H.; Yan, Q.; Chen, H. Reducing the Symmetry of Bimetallic Au@Ag Nanoparticles by Exploiting Eccentric Polymer Shells. *J. Am. Chem. Soc.* **2010**, *132*, 9537–9539.
14 Wong, Y. J.; Zhu, L.; Teo, W. S.; Tan, Y. W.; Yang, Y.; Wang, C.; Chen, H. Revisiting the Stöber Method: Inhomogeneity in Silica Shells. *J. Am. Chem. Soc.* **2011**, *133*, 11422–11425.
15 Zhu, L.; Wang, H.; Shen, X.; Chen, L.; Wang, Y.; Chen, H. Developing Mutually Encapsulating Materials for Versatile Syntheses of Multilayer Metal–Silica–Polymer Hybrid Nanostructures. *Small* **2012**, *8*, 1857–1862.
16 Guerrero-Martinez, A.; Perez-Juste, J.; Liz-Marzan, L. M. Recent Progress on Silica Coating of Nanoparticles and Related Nanomaterials. *Adv. Mater.* **2010**, *22*, 1182–1195.
17 Casavola, M.; Buonsanti, R.; Caputo, G.; Cozzoli, P. D. Colloidal Strategies for Preparing Oxide-Based Hybrid Nanocrystals. *Eur. J. Inorg. Chem.* **2008**, 837–854.
18 Carbone, L.; Cozzoli, P. D. Colloidal Heterostructured Nanocrystals: Synthesis and Growth Mechanisms. *Nano Today* **2010**, *5*, 449–493.
19 Zhang, H.; Li, Y.; Ivanov, I. A.; Qu, Y.; Huang, Y.; Duan, X. Plasmonic Modulation of the Upconversion Fluorescence in NaYF4:Yb/Tm Hexaplate Nanocrystals Using Gold Nanoparticles or Nanoshells. *Angew. Chem., Int. Ed.* **2010**, *49*, 2865–2868.
20 Brinson, B. E.; Lassiter, J. B.; Levin, C. S.; Bardhan, R.; Mirin, N.; Halas, N. J. Nanoshells Made Easy: Improving Au Layer Growth on Nanoparticle Surfaces. *Langmuir* **2008**, *24*, 14166–14171.
21 Wang, Y.; Wang, Q.; Sun, H.; Zhang, W.; Chen, G.; Wang, Y.; Shen, X.; Han, Y.; Lu, X.; Chen, H. Chiral Transformation: From Single Nanowire to Double Helix. *J. Am. Chem. Soc.* **2011**, *133*, 20060–20063.

22 Mulvaney, S. P.; Musick, M. D.; Keating, C. D.; Natan, M. J. Glass-Coated, Analyte-Tagged Nanoparticles: A New Tagging System Based on Detection with Surface-Enhanced Raman Scattering. *Langmuir* **2003**, *19*, 4784–4790.

23 Yang, M.; Chen, T.; Lau, W. S.; Wang, Y.; Tang, Q.; Yang, Y.; Chen, H. Development of Polymer-Encapsulated Metal Nanoparticles as Surface-Enhanced Raman Scattering Probes. *Small* **2009**, *5*, 198–202.

24 Yang, M.; Chen, G.; Zhao, Y.; Silber, G.; Wang, Y.; Xing, S.; Han, Y.; Chen, H. Mechanistic Investigation into the Spontaneous Linear Assembly of Gold Nanospheres. *Phys. Chem. Chem. Phys.* **2010**, *12*, 11850–11860.

25 Feng, Y.; Wang, Y.; Wang, H.; Chen, T.; Tay, Y. Y.; Yao, L.; Yan, Q.; Li, S.; Chen, H. Engineering "Hot" Nanoparticles for Surface-Enhanced Raman Scattering by Embedding Reporter Molecules in Metal Layers. *Small* **2012**, *8*, 246–251.

26 Wang, X.; Li, G.; Chen, T.; Yang, M.; Zhang, Z.; Wu, T.; Chen, H. Polymer-Encapsulated Gold-Nanoparticle Dimers: Facile Preparation and Catalytical Application in Guided Growth of Dimeric ZnO-Nanowires. *Nano Lett.* **2008**, *8*, 2643–2647.

27 Chen, G.; Wang, Y.; Yang, M.; Xu, J.; Goh, S. J.; Pan, M.; Chen, H. Measuring Ensemble-Averaged Surface-Enhanced Raman Scattering in the Hotspots of Colloidal Nanoparticle Dimers and Trimers. *J. Am. Chem. Soc.* **2010**, *132*, 3644–3645.

28 Chen, G.; Wang, Y.; Tan, L. H.; Yang, M.; Tan, L. S.; Chen, Y.; Chen, H. High-Purity Separation of Gold Nanoparticle Dimers and Trimers. *J. Am. Chem. Soc.* **2009**, *131*, 4218–4219.

29 Shen, X.; Chen, L.; Li, D.; Zhu, L.; Wang, H.; Liu, C.; Wang, Y.; Xiong, Q.; Chen, H. Assembly of Colloidal Nanoparticles Directed by the Microstructures of Polycrystalline Ice. *ACS Nano* **2011**, *5*, 8426–8433.

30 Sindoro, M.; Feng, Y.; Xing, S.; Li, H.; Xu, J.; Hu, H.; Liu, C.; Wang, Y.; Zhang, H.; Shen, Z.; Chen, H. Triple-Layer (Au@Perylene)@Polyaniline Nanocomposite: Unconventional Growth of Faceted Organic Nanocrystals on Polycrystalline Au. *Angew. Chem., Int. Ed.* **2011**, *50*, 9898–9902.

31 Pan, M.; Xing, S.; Sun, T.; Zhou, W.; Sindoro, M.; Teo, H. H.; Yan, Q.; Chen, H. 3D Dendritic Gold Nanostructures: Seeded Growth of a Multi-generation Fractal Architecture. *Chem. Commun.* **2010**, *46*, 7112–7114.

32 Pan, M.; Sun, H.; Lim, J. W.; Bakaul, S. R.; Zeng, Y.; Xing, S.; Wu, T.; Yan, Q.; Chen, H. Seeded Growth of Two-dimensional Dendritic Gold Nanostructures. *Chem. Commun.* **2012**, *48*, 1440–1442.

33 Wang, H.; Chen, L.; Shen, X.; Zhu, L.; He, J.; Chen, H. Unconventional Chain-Growth Mode in the Assembly of Colloidal Gold Nanoparticles. *Angew. Chem., Int. Ed.* **2012**, *51*, 8021–8025.

34 Xu, J.; Wang, H.; Liu, C.; Yang, Y.; Chen, T.; Wang, Y.; Wang, F.; Liu, X.; Xing, B.; Chen, H. Mechanical Nanosprings: Induced Coiling and Uncoiling of Ultrathin Au Nanowires. *J. Am. Chem. Soc.* **2010**, *132*, 11920–11922.

35 Chen, L.; Wang, H.; Xu, J.; Shen, X.; Yao, L.; Zhu, L.; Zeng, Z.; Zhang, H.; Chen, H. Controlling Reversible Elastic Deformation of Carbon Nanotube Rings. *J. Am. Chem. Soc.* **2011**, *133*, 9654–9657.

36 Chen, L.; Yu, S.; Wang, H.; Xu, J.; Liu, C.; Chong, W. H.; Chen, H. General Methodology of Using Oil-in-Water and Water-in-Oil Emulsions for Coiling Nanofilaments. *J. Am. Chem. Soc.* **2012**, *135*, 835–843.

37 Zhu, L.; Shen, X.; Zeng, Z.; Wang, H.; Zhang, H.; Chen, H. Induced Coiling Action: Exploring the Intrinsic Defects in Five-Fold Twinned Silver Nanowires. *ACS Nano* **2012**, *6*, 6033–6039.

38 Wang, Y.; Chen, G.; Yang, M.; Silber, G.; Xing, S.; Tan, L. H.; Wang, F.; Feng, Y.; Liu, X.; Li, S.; Chen, H. A Systems Approach Towards the Stoichiometry-controlled Hetero-assembly of Nanoparticles. *Nat. Commun.* **2010**, *1*, 87.

39 Wang, H.; Xu, J.; Wang, J.; Chen, T.; Wang, Y.; Tan, Y. W.; Su, H.; Chan, K. L.; Chen, H. Probing the Kinetics of Short-Distance Drug Release from Nanocarriers to Nanoacceptors. *Angew. Chem., Int. Ed.* **2010**, *49*, 8426–8430.

40 Sun, H.; Shen, X.; Yao, L.; Xing, S.; Wang, H.; Feng, Y.; Chen, H. Measuring the Unusually Slow Ionic Diffusion in Polyaniline via Study of Yolk-Shell Nanostructures. *J. Am. Chem. Soc.* **2012**, *134*, 11243–11250.